Received: 14 June 2017 | Revised: 17 November 2017 | Accepted: 28 December 2017

DOI: 10.1002/ldr.2882

RESEARCH ARTICLE

WILEY

Dynamic monitoring of soil erosion in the upper Minjiang catchment using an improved soil loss equation based on remote sensing and geographic information system

Bing Guo[1,2,4,5,6] | Guang Yang[3] | Feifei Zhang[3] | Fang Han[1] | Chenggang Liu[7]

[1] School of Civil and Architectural Engineering, Shandong University of Technology, Zibo 255000, P. R. China

[2] Key Laboratory of Geographic Information Science (Ministry of Education), East China Normal University, Shanghai 200241, P. R. China

[3] Institute of Remote Sensing and Digital Earth, Chinese Academy of Sciences, Beijing 100101, P. R. China

[4] Key Laboratory for National Geographic Census and Monitoring, National Administration of Surveying, Mapping and Geoinformation, Wuhan 433079, P. R. China

[5] Key Laboratory for Digital Land and Resources of Jiangxi Province, East China University of Technology, Nanchang 330013, P. R. China

[6] Hubei Key Laboratory of Regional Development and Environmental Response (Hubei University), Wuhan 430062, P. R. China

[7] Key Laboratory of Tropical Plant Resources and Sustainable Use, Xishuangbanna Tropical Botanical Garden, Chinese Academy of Sciences, Menglun 666303, P. R. China

Correspondence

G. Yang, Institute of Remote Sensing and Digital Earth, Chinese Academy of Sciences, Datun Road 20, Chaoyang District, Beijing 100101, P. R. China.
Email: yangguang@radi.ac.cn

F. Zhang, Institute of Remote Sensing and Digital Earth, Chinese Academy of Sciences, Datun Road 20, Chaoyang District, Beijing 100101, China.
Email: zhangfeifei@radi.ac.cn

Funding information

Project of Hubei Key Laboratory of Regional Development and Environmental Response (Hubei University), Grant/Award Number: 2017(B)003; Open Fund of Key Laboratory for National Geographic Census and Monitoring, National Administration of Surveying, Mapping and Geoinformation, Grant/Award Number: 2016NGCM02; Open Fund of Key Laboratory for Digital Land and Resources of Jiangxi Province, East China University of Technology, Grant/Award Number: DLLJ201709; Open Fund of Key Laboratory of Geographic Information Science (Ministry of Education), East China Normal University, Grant/Award Number: KLGIS2017A02

Abstract

The upper Minjiang catchment has suffered intensive soil erosion due to frequent geologic hazards and its fragile ecosystem zone with steep slopes. This study fully considers the topographic features and surface cover and introduces improved methods of *K*, *LS*, and *C* to establish a soil loss equation for the upper Minjiang catchment based on remote sensing and geographic information system. Spatial–temporal change patterns of soil erosion intensity and its driving mechanisms are then analyzed and discussed. Results show that (a) the soil erosion modulus of the upper Minjiang catchment for 2005 and 2015 were 1,577.29 t km^{-2} a^{-1} and 1,619.77 t km^{-2} a^{-1}, both of which belong to a level of mild erosion. The slight and mild erosion zones covered the largest area and were widely distributed in the northern part of the study area, whereas zones of intensive and severe erosion were mostly concentrated in Wenchuan County and the lower reaches of the Heishui and Zagunao Rivers. (b) During 2005–2015, changes in erosion intensity showed a trend of "overall stability, local deterioration." Zones of mild, moderate, and intensive increase were mainly concentrated in the Longmen Mountain Fault Zone, such as southern Maoxian and western Wenchuan Counties. (c) Returning cultivated land to forest and grasslands greatly reduced the erosion intensity and erosion amount, whereas geologic hazards aggravated the soil erosion condition. Zones with a slope of <35° had a positive relationship with soil erosion intensity; these areas are crucial control areas for soil preservation and containing soil loss. In addition, grassland is more effective in conserving soil and water than forestland in the upper Minjiang catchment in areas of steep terrain. These results provide an important reference for estimating soil loss intensity in southwest mountainous regions of China, particularly in the Hengduan Mountains, and greatly contribute to the planning of soil and water conservation.

KEYWORDS

driving factors, dynamic monitoring, RS, soil loss equation, the upper Minjiang catchment

1 | INTRODUCTION

Soil is important for maintaining the normal operation of surface ecosystems. Areas of soil erosion negatively impact local ecology, leading to a deterioration in water quality, lowering effective levels of reservoir water, reducing crop productivity, and enabling flooding and habitat destruction (B. Guo, Tao, Liu, & Jiang, 2012; Shi, Cai, Ding, Li, & Wang, 2002). In relation to the increasing effects of global

warming and human disturbance, soil erosion has become one of the largest and most widespread environmental threats that greatly affect the sustainable development of regional and national social economies (B. Guo et al., 2012; Y. Q. Xu, Shao, Kong, Peng, & Cai, 2008). Under the influence of heavy precipitation and steep slope, the geologic hazards, including landslide, debris flow, and collapse, occur frequently, which leads to serious soil erosion in the upper Minjiang catchment. Moreover, the deforestation and reclamation have accelerated the condition of the soil and water loss. It is thus of considerable importance to quantitatively evaluate the soil loss rate by water and to analyze associated spatial–temporal change patterns for the upper Minjiang catchment.

The process of soil erosion is mainly controlled by natural and human factors such as soil texture, soil physical and chemical composition, climate (precipitation), terrain (slope, aspect, and shape), ground cover (vegetation coverage [VC] and land use types), and any interactions between them (Koiter, Owens, Petticrew, & Lobb, 2017; Z. W. Li et al., 2017; Wei, Zhang, McLaughlin, et al., 2017). Substantial efforts have been made to develop quantitative assessment models of soil erosion, and those developed mainly belong to two categories, either on-site measurements that are often applied in small-scale regional or point experiments or off-site quantification models, which can be used to evaluate the erosion intensity of zones on a large scale (Ganasri & Ramesh, 2016; Tamene, Park, Dikau, & Vlek, 2006; L. F. Xu, Xu, & Meng, 2013). Models developed to date to quantify soil erosion such as the Universal Soil Loss Equation (USLE; Mattheus & Norton, 2015), the Water Erosion Prediction Project (Baigorria & Romero, 2007), the European Soil Erosion Model (Khaleghpanah, Shorafa, Asadi, Gorji, & Davari, 2016), and the Erosion for Agricultural Management System (Vanwalleghem et al., 2017) are considered to be the most scientific approaches for use in studies, although experimental measurements are still considered indispensable and fundamental (Brooks, Dobre, Elliot, Wu, & Boll, 2016; Kinnell, 2017).

In addition, the Revised Universal Soil Loss Equation (RUSLE) has better application in zones on different scales and with differing ecosystems (Prasannakumar, Vijith, Abinod, & Geetha, 2012). With the development of aerospace and computer technologies, an increasing number of studies have therefore combined RUSLE and USLE with 3S (geographic information system [GIS], remote sensing [RS], and Global Positioning System) to examine soil loss rate on different temporal–spatial scales. For example, the spatial–temporal change patterns of soil erosion intensity (SEI) of the Minjiang catchment during 1995–2005 were analyzed with the combination of RS, GIS, and RUSLE (Deng, Meng, Wang, & Liu, 2008). Y. Liu, Li, and Long (2009) quantitatively examined the SEI of Minjiang headwater region utilizing GIS and RS and then analyzed the relationship between agroforest landscape and SEI. L. Jiang et al. (2014) analyzed the spatial and temporal change patterns of soil erosion in the upper Minjiang catchment during 2005–2010 utilizing GIS, RS, and RUSLE. The comprehensive applications of ^{137}Cs, RS, and GIS technology have also been applied to assess soil erosion in the Xiaojiang watershed of Yunnan Province, which has been proven to be an efficient model for the western mountains of China, particularly for zones where observation data are scare and the USLE is not suitable for use (Ge, Cui, Lin, Zhuang, & Jia, 2014). However, previous studies mostly focused on the SEI of regions with minor slopes (<10°) and have paid less attention to mountain areas with steeper slopes (>25°; L. Jiang et al., 2014). Most studies have directly calculated the amount of soil erosion using factor formulas of length-slope (*LS*) and *C* derived from USLE and have thus ignored the effects of steep slope (>25°) and distinct land cover in mountainous areas (Fu et al., 2005; Y. Q. Xu et al., 2008).

In view of the shortcomings mentioned above, this paper improves calculation methods for *LS*, *K*, and *C* and develops a soil loss equation for the upper Minjiang catchment, in consideration of the regional terrain and geographical conditions based on RS and GIS. This study therefore provides answers to four core research questions, listed as follows. (a) How much soil has been lost (t km^{-2} a^{-1}) in the upper Minjiang catchment? (b) What are the spatial–temporal change distribution patterns of soil loss intensity in the upper Minjiang catchment? (c) What are the relationships between soil loss intensity and slope, plant types, and VC? (d) How did geologic hazards and the policies of returning farmland to forest and grassland effect changes in soil erosion during 2005–2015? The results thus provide an important reference for estimating soil erosion in the mountainous areas of Southwest China, particularly in the Hengduan Mountains, and then contribute to the controls and prevention of soil erosion.

2 | MATERIALS AND METHODS

2.1 | Study area description

The upper Minjiang catchment is located in western Sichuan (China) in an area of high mountains (31°–33°N, 102°–104°E) and spans five counties (Songpan, Heishui, Maoxian, Lixian, and Wenchun, as shown in Figure 1; L. Jiang et al., 2014). This basin covers an area of about 2.4×10^4 km^2 and is characterized by complex eco-environmental conditions. The mean annual precipitation is 490.7–835.8 mm and the average temperature ranging from −7.4 to 22.7 °C (A. N. Li, Wang, Liang, & Zhou, 2006). The main soil types include alfisol, brown forest soil, and cinnamon soil, all of which contain large quantities of gravel and large stone-sand pores that provide good penetrability (W. G. Zhang, Hu, et al., 2008). The plant species in this basin vary significantly with elevation and include *Picea* spp., *Larix* spp., *Abies* spp., *Cupressus funebris*, and *Betula* spp. (Fang, Fan, Shen, & Song, 2014). The upper Minjiang catchment is represented by complicated landforms, rich biological species, and diversified climate types, and as such, this unique area offers the opportunity to study ecosystems in mountainous areas of southwest China (Hong et al., 2007).

2.2 | Data collection and processing

MODIS normal differential vegetation index (NDVI) time series data for 2005 and 2015 (h25v05 and h26v05) are derived from the National Aeronautics and Space Administration Earth Observing System at a spatial resolution of 250 m with 15-day intervals (Al-Hamdan et al., 2017). The reprojection (from sinusoidal projection to WGS84/Albers projection), format conversion (from HDF to GeoTIFF), and images mosaic for the above datasets are conducted with the tool of MODIS Reprojection Tool. Then, the monthly NDVI is obtained based on the dataset of semimonthly NDVI utilizing the method of maximum value

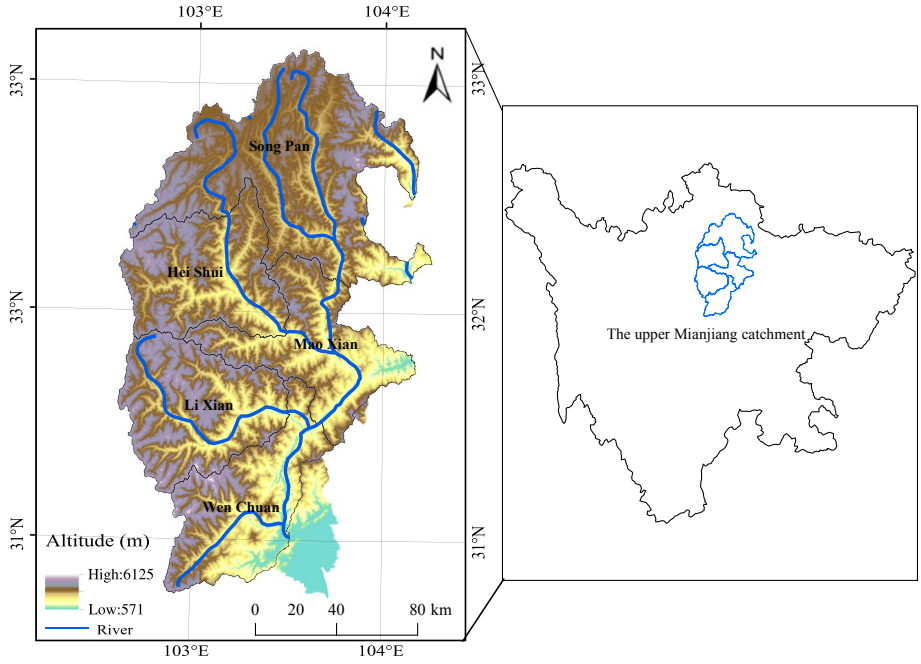

FIGURE 1 Location of the upper Minjiang catchment with topography [Colour figure can be viewed at wileyonlinelibrary.com]

composite. Meteorological data of daily precipitation used in this study are obtained from the China Meteorological Administration, and the interpolation method of Cokriging is applied for the data spatializations of meteorological factors with ArcGIS 10.2. The dataset of the 90-m digital elevation model is obtained from the National Geospatial-Intelligence Agency–National Aeronautics and Space Administration, which is used to generate the geomorphologic parameters (slope and slope length). In addition, data of soil organic carbon and soil particle size distribution (including sand fraction, silt fraction, and clay fraction) are obtained from National Earth System Science Data Sharing Infrastructure, at a spatial resolution of 1,000 m. Land use types in 2005 and 2015 (available at http://www.geodata.cn/, with a spatial resolution of 100 m) are obtained from National Earth System Science Data Sharing Infrastructure. All the above datasets and secondary data are then reprojected to the WGS84/Albers projection with a spatial resolution of 250 m, thereby providing convenient data for discussion and analysis and use in subsequent research.

2.3 | Soil loss equation of the upper Minjiang catchment

The model of USLE is based on large numbers of observed and simulated rainfall data and has been widely applied in regions with different environmental conditions throughout the world since its establishment in 1965. However, as the model only considers rainfall erosivity, experts and scholars have proposed a model of RUSLE based on USLE (H. Chen, Oguchi, & Wu, 2017). Other researchers have also established and developed domestic models and equations based on models of USLE and RUSLE, which consider certain unique regional ecological characteristics, such as the Soil Loss Equation for the Area Affected by 4·20 Lushan Earthquake (B. T. Liu, Song, Shi, & Tao, 2016), the Soil Loss Equation for China (Cheng, Yang, Xie, Wang, & Guo, 2009; W. B. Zhang & Liu, 2003), the Soil Loss Equation for Heilongjiang Province (B. Guo et al., 2012), the Soil Loss Equation for Jinsha River Basin of Yunnan Province (B. T. Liu et al., 2016), and the Soil Loss Equation for Beijing (B. Y. Liu, Bi, & Fu, 2010). In this paper, the Soil Loss Equation for the Upper Reaches of Minjiang is developed based on RUSLE (a monthly model), which better reflects the temporal imbalance of precipitation and seasonal changes of vegetation growth in 1 year (L. Jiang et al., 2014). The formula is as follows:

$$A = K{\cdot}L{\cdot}S{\cdot}P{\cdot}\sum_{i=1}^{12} R_i{\cdot}C_i, \tag{1}$$

where A refers to the rate of soil loss for a certain period (t km^{-2} a^{-1}), K refers to the soil erodibility (t km^2 h km^{-2} h^{-1} mm^{-1}), L refers to the slope length factors (dimensionless), S refers to the slope steepness factor (dimensionless), P refers to the erosion support practice or land management factor (dimensionless, 0–1), R_i refers to the rainfall erosivity factor of month i (MJ mm km^{-2} h^{-1} m^{-1}), and C_i is the cover and management factor of month i (dimensionless, 0–1).

2.4 | Calculation of factors

1. Rainfall erosivity (R)

The factor of R indicates the potential capacity of soil erosion related to rainfall, which is obtained with detailed, continuous precipitation data (L. Jiang et al., 2014). R is a better indicator of the two key features of a rainstorm that determines its erosivity by amount of precipitation and peak precipitation intensity during certain period (Y. Q. Xu, Shao, & Peng, 2009). It thus reflects the driving force factor for soil erosion and has a significant relationship with total rainfall and rainfall intensity (Xie, Yin, Liu, Nearing, & Zhao, 2016). In most research, the monthly or annual rainfall is utilized to calculate rainfall erosivity. However, it is difficult to provide detailed rainfall information on a daily time scale due to time limitations involved, and such

methods are thus not efficient in calculating the rainfall erosivity factor (Xie et al., 2016). Therefore, in this paper, the daily rainfall model proposed by Xie et al. (2016) is applied to calculate rainfall erosivity based on data from 65 meteorological stations. *R* factors of 2005 and 2015 are then calculated utilizing the interpolation method of Cokriging with a spatial resolution of 250 m. The equation used to obtain the *R* factor is as follows:

$$\begin{aligned}&\overline{R_k} = \frac{1}{N}\sum_{i=1}^{N}\left(\alpha\sum_{j=1}^{m}P^{\beta}{}_{dijk}\right),\\&\alpha = 21.239\beta^{-7.3967}\ \beta = 0.6243 + \frac{27.346}{\overline{P_{d12}}},\\&\overline{P_{d12}} = \frac{1}{N}\sum_{i=1}^{N}\frac{1}{m}\sum_{l=1}^{n}P_{il},\\&i = 1,2\ldots,N j = 1,2\ldots.m l = 1,2\ldots n,\end{aligned} \tag{2}$$

where $\overline{R_k}$ is rainfall erosivity (MJ mm km^{-2} h^{-1} m^{-1}), *n* refers to the length of the time series, *m* is the number of days for month *k* in year *i* with erosive rainfall, P_{dijk} is the *j* erosive rainfall for month *k* in year *i* (mm), α, β refer to the parameters of the model, $\overline{P_{d12}}$ is the average erosive precipitation (mm), and daily rainfall over 12 mm is defined as the erosive precipitation.

2. Soil erodibility (*K*)

Soil erodibility (*K*) represents the response sensitivity of soil mass to the effects of rainfall splash or surface runoff denudation and transportation and has a significant relationship with soil particle size, soil texture, and rainfall (Lee & Lee, 2006; Xiao et al., 2017). The environmental policy-integrated climate (EPIC) is one of the methods used to calculate soil erodibility and is widely used in many studies:

$$\begin{aligned}K_{\mathrm{EPIC}} =&\left\{0.2 + 0.3\exp\left[-0.0256S_{\mathrm{a}}\left(1\text{-}\frac{S_i}{100}\right)\right]\right\}\left(\frac{S_i}{C_l + S_i}\right)^{0.3}\\&\times\left[1 - \frac{0.25C_0}{C_0 + \exp(3.72 - 2.95C_0)}\right]\\&\times\left[1 - \frac{0.7Sn}{Sn + \exp(-5.51 + 22.9Sn)}\right], S_n = 1 - S_a/100\ ,\end{aligned} \tag{3}$$

where K_{EPIC} is soil erodibility, S_a refers to sand content (%), S_i refers to silt content (%), C_l refers to clay content (%), and C_0 refers to the organic carbon content (%).

However, K. L. Zhang, Shu, Xu, Yang, and Yu (2008) found a large difference between the reversed value using the EPIC model and actual measured *K* values in different regions, and thus a modified formula of *K* was proposed as

$$K_M = -0.01383 + 0.51575K_{\mathrm{EPIC}}. \tag{4}$$

3. Slope length and steepness factor (*LS*)

The topographic factor refers to the soil loss ratio under given condition to that at a field site with a "standard" slope length of 22.6 m and slope steepness of 9% (Dabral, Baithuri, & Pandey, 2008). Topography and geomorphology play an important role in affecting the process of soil erosion and the subsequent application of soil conservation measures, which is composed of slope length (*L*) and slope steepness (*S*; K. Liu, Tang, Zhu, Yang, & Song, 2015). *L* indicates the influence of slope length on erosion whereas *S* reflects the effects of slope steepness on erosion (L. Jiang et al., 2014). Soil loss is greater with steeper slopes and longer lengths as runoff energy is increased (Y. Liu et al., 2009). Based on the original method of *LS* in USLE and RUSLE, a number of researchers in China have developed algorithms for different research areas that fully consider topographic features, such as the Yang Zisheng algorithm (B. T. Liu et al., 2016) for the Jinsha River Basin and the Liu Baoyuan algorithm (W. B. Zhang & Liu, 2003). In the upper Minjiang catchment, 50% of the basin consists of zones with slopes of >25° and topographic characteristics similar to those of the Jinsha River Basin. Therefore, the *L* from the Yang Zisheng algorithm for the Jinsha River Basin is applied in this paper as

$$L = \left(\frac{L_0}{20}\right)^{0.24}, \tag{5}$$

where *L* represents the factor of slope length and L_0 refers to the length of watershed (m).

With knowledge of the steep terrain of the upper Minjiang catchment and observed data of the watershed, a method to determine the slope factor of steep slopes is introduced with the formula as follows:

$$S = \begin{cases}10.8\sin\theta + 0.03 & \theta < 5^{\circ}\\16.8\sin\theta - 0.5 & 5^{\circ} < \theta \le 10^{\circ}\\20.204\sin\theta - 1.2404 & 10^{\circ} < \theta \le 25^{\circ}\\29.585\sin\theta - 5.6079 & \theta > 25^{\circ}\end{cases} \tag{6}$$

where *S* is the slope steepness factor and θ is the slope (°).

4. Cover and management factor (*C*)

The factor of *C* refers to the ratio of soil loss between a soil surface covered with vegetation and a completely exposed soil surface under the same conditions and its value ranges from 0 to 1 (Q. K. Guo, Liu, Xie, Liu, & Yin, 2015). The current calculation methods used to determine *C* are mainly composed of watershed observations, artificial assignments, and the RS inversion method based on VC (Z. S. Jiang & Zheng, 2004). The upper Minjiang catchment is located in the regions of Hengduan Mountain with steep terrain; the area is thus not easily accessible to conduct field observations and obtain associated data. Therefore, in this study, the RS inversion method based on VC is used to obtain the *C* factor.

Forests and grasslands are widely distributed within the upper Minjiang catchment (accounting for more than 70% of the entire region). The method proposed by H. Chen, Oguchi, & Wu (2017) aims to invert the *C* factor for forest, whereas that of L. Jiang et al. (2014) calculates the *C* value for grassland based on the NDVI. Both methods have been widely used in many studies, and the associated equations are as follows:

$$C_{\mathrm{grass}} = \begin{cases}1.0 & fc \le 5\%\\e^{-0.0418(fc-5)} & fc > 5\%\end{cases}, \tag{7}$$

$$C_{\mathrm{forest}} = \exp\left[-\alpha\cdot\frac{NDVI}{(\beta - NDVI)}\right], \tag{8}$$

where C_{grass} is the cover and management factor for grassland, *fc* is VC, C_{forest} refers to the cover and management factor for forest, NDVI is the normal differential vegetation index, and α,β are the model parameters.

5. Erosion support practice or land management factor (*P*)

The erosion support practice or land management factor (*P*) refers to the area ratio between actual erosion and standard erosion under the same conditions (B. T. Liu et al., 2016). The factor of *P* accounts for erosion support practices, which can reduce the erosion intensity of the runoff by the influence on runoff concentration and runoff velocity (B. Guo et al., 2012). The value of *P* ranges from 0 to 1, where 0 indicates no soil erosion and 1 means that soil and water conservancy measures have no effect on soil loss (common soil and water conservation measures include level terracing, slope terracing, and contour strip cropping). Because of the lack of observed data for the upper Minjiang catchment, the value of *P* is calculated with the achievements of previous researches and the first national soil and water conservation census (Deng et al., 2008; L. Jiang et al., 2014). The *P* value is assigned for each type of land use (Table 1).

3 | RESULTS

3.1 | Spatial patterns of different SEIs in 2005 and 2015

The above six erosion factors are integrated to calculate the SEI for 2005 and 2015, based on the soil loss equation for the upper Minjiang catchment. The SEI is then divided into five categories using the SL-190-2007 "classification standard of water erosion intensity in classification of soil erosion" (B. Guo et al., 2012; L. F. Xu et al., 2013), where SEI < 500 t km^{-2} a^{-1} is slight erosion, 500 t km^{-2} a^{-1} ≤ SEI < 2,500 t km^{-2} a^{-1} is mild erosion, 2,500 t km^{-2} a^{-1} ≤ SEI < 5,000 t km^{-2} a^{-1} is moderate erosion, 5,000 t km^{-2} a^{-1} ≤ SEI < 8,000 t km^{-2} a^{-1} is intensive erosion, and SEI > 8,000 t km^{-2} a^{-1} is severe erosion. The spatial–temporal change patterns of soil erosion are then analyzed (Figure 2).

In order to validate the precision of the estimated results, we have chosen 254 field sites from zones with different eco-environmental characteristics in 2015 (Table 2). The data of field observed SEIs were obtained from First National Census for Soil and Water conservation, which included the erosion rate (t km^{-2} a^{-1}) and soil loss thickness(mm a^{-1}). According to the "classification criteria for SEI (SL190-2007; Ministry of Water Resource of the People's Republic of China 2007)," the field observed SEIs were graded (Table 3).

The evaluated erosion results are in consistency with the field observed results, which is indicated by an overall accuracy of 91.3%. Thus, the improved model proposed in this study has better applicability in the upper Minjiang catchment.

As shown in Figure 2 and Table 4, the total amount of soil erosion in the upper Minjiang catchment in 2005 was 3,888 × 10^4 t, and the soil erosion modulus was 1,577.29 t km^{-2} a^{-1}, which equates to a level of mild erosion. However, significant differences in the spatial distribution existed among different erosion intensity levels. The largest category was that of mild erosion, which covered an area of 10,595.00 km^2 (accounting for 42.98%) and was mostly distributed in Songpan and Heishui Counties. The second largest category was that of slight erosion, covering an area of 8,345.75 km^2 and accounting for 33.86% of the study region; followed by moderate erosion covering an area of 4,582.75 km^2 and accounting for 18.59% of the total area. Slight erosion was discontinuously distributed in the river valleys of the Heishui, Maoergai, and Baicao Rivers, whereas the moderate erosion zone was mostly concentrated in the northern part of Lixian and eastern Maoxian Counties. Intensive and severe erosion zones covering areas of 1,064.94 and 61.56 km^2, respectively, were mainly concentrated in Wenchuan County and the lower reaches of the Heishui River and Zagunao River.

As shown in Figure 3, with respect to erosion quantities and ratios, moderate erosion represented the largest amount of erosion at 1,597.82 × 10^4 t (accounting for 41.10%) followed by mild erosion with an erosion quantity of 1,450.07 × 10^4 t, whereas severe erosion represented the smallest erosion quantity with 54.45 × 10^4 t, although its erosion rate was the largest at 8,844.76 t km^{-2} a^{-1}.

In 2015, the total quantity of soil eroded in the upper Minjiang catchment was 3,992 × 10^4 t, with a soil erosion modulus of 1,619.77 t km^{-2} a^{-1}, and this amount was associated with a mild level of erosion. However, there were significant spatial disparities between soil erosion zones (Table 4). Of all the erosion intensity levels, the zone of mild erosion covered the largest area (11,522.75 km^2), accounting for 46.75% of the study region. Zones of slight, moderate, and intensive erosion were 7,102.06, 5,249.88, and 759.31 km^2, respectively. However, the severe erosion had the smallest area of 16.00 km^2. Slight and mild erosion were mostly distributed in the northern part of the upper Minjiang catchment, whereas zones of intensive and severe erosion were discontinuously distributed in Wenchuan County and the lower reaches of the Heishui and Zagunao Rivers. With respect to the quantity of erosion, the zone where moderate erosion occurred was the largest at 1,822.45 × 10^4 t, followed by the mild erosion zone (1,570.25 × 10^4 t) and the intensive erosion zone (438.67 × 10^4 t).

3.2 | Spatial patterns differences for erosion intensity among different land use types

As shown in Figure 4, the spatial disparities of all grades of SEIs differ significantly. In 2005, the slight and mild erosion zones were the largest for cultivated land, forest, and shrub, accounting for 100.00%, 95.94%, and 94.52% of these areas, respectively. Mild and moderate erosion zones were widely distributed in meadow and grassland, accounting for 86.70% and 89.55% of these areas, respectively.

TABLE 1 Values of *P* for different land use types

Land use types	Paddy	Dry	Forest	Grassland	Water	Residential	Rocky	Swamp	Others
P	0.05	0.35	1	1	0	0	0	0.01	1

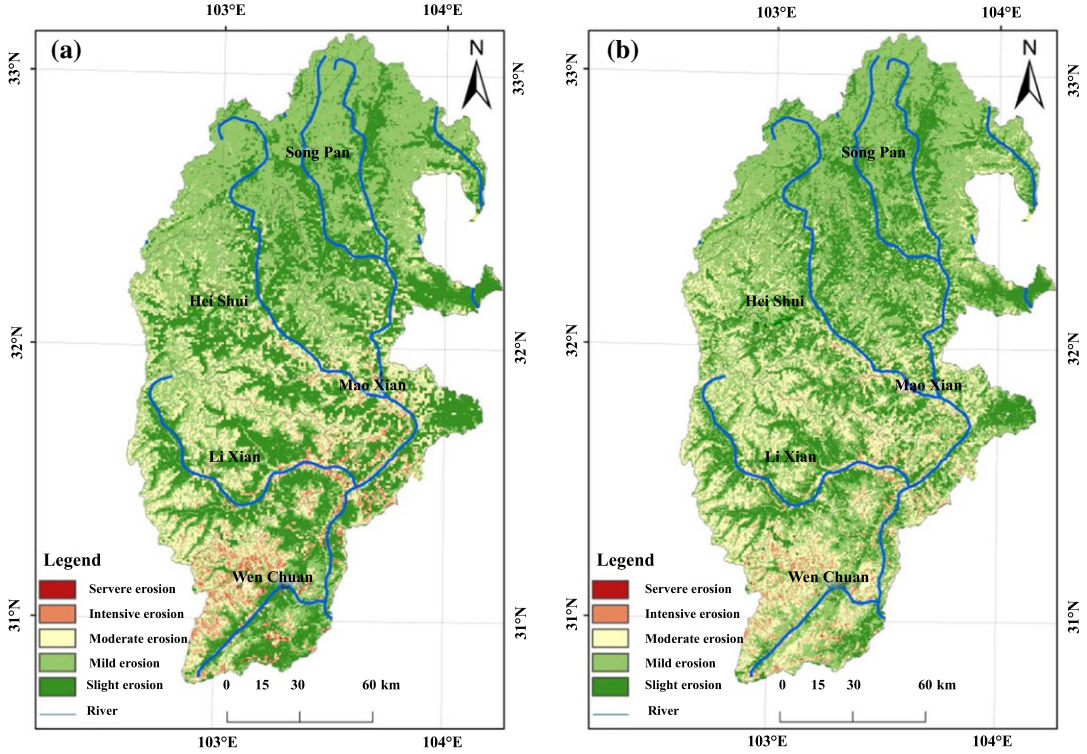

FIGURE 2 Spatial patterns of soil erosion intensity for 2005 and 2015 in the upper Minjiang catchment. (a) Soil erosion intensity for 2005. (b) Soil erosion intensity for 2015 [Colour figure can be viewed at wileyonlinelibrary.com]

TABLE 2 Distribution of field observation points of soil erosion

Observed erosion severity	Evaluating results of soil erosion					
	Slight	Mild	Moderate	Intensive	Severe	Sum
Slight	73	1	1	0	0	75
Mild	2	80	2	1	0	85
Moderate	1	2	34	0	0	37
Intensive	0	1	1	31	4	37
Severe	1	0	0	5	14	20
Sum	77	84	38	37	18	254

However, in 2015, cultivated land, forest, and shrub were mainly dominated by slight and mild erosion zones, whereas mild and moderate erosion were the main grades in meadow and grasslands.

To monitor changes in SEIs among the typical land use types, the SEI index (SEII; Equation 9; L. Jiang et al., 2014) is applied to analyze the relationships between SEI and land use types:

$$W_j = 100 \times \sum_{i=1}^{n} R_i \times P_{ij} \quad (9)$$

TABLE 3 Classification criteria for field observed soil erosion intensity

Erosion categories	Erosion rate (t km^{-2} a^{-1})	Soil loss thickness (mm a^{-1})
Slight erosion	<200, 500, 1,000	<0.15, 0.37, 0.74
Mild erosion	200, 500, 1,000–2,500	0.15, 0.37, 0.74–1.9
Moderate erosion	2,500–5,000	1.9–3.7
Intensive erosion	5,000–8,000	3.7–5.9
Severe erosion	>8,000	>5.9

where W_j index refers to the SEI index for land use type of j; R_i refers to the category level value of i for the land use type of j; and P_{ij} refers to the area percentage of category level i for land use type of j.

As shown in Figures 4 and 5, there was an increasing trend in the SEII for paddy field, dryland, forest, and shrub during 2005–2015, with increasing magnitudes of 39.73, 21.89, 12.51, and 14.52, respectively. This occurred in relation to the expansion of mild and moderate erosion zones and a reduction in the size of slight erosion zones. In addition, the change in the erosion intensity in grassland and meadow showed a stable trend with smaller changes in the SEII; this is related to the minimal changes in areas of mild, moderate, and intensive erosion.

3.3 | Change in patterns of SEI during 2005–2015

To efficiently monitor the spatial–temporal changes in the SEI, the change intensity (CI) is calculated for 2005 and 2015 (Figure 6). By considering the eco-environmental characteristics, the CI was graded into seven levels based on the standard deviation and histogram distribution of images: intensive decrease (CI < −3,825 t km^{-2} a^{-1}), moderate decrease (−3,825 t km^{-2} a^{-1} ≤ CI < −2,550 t km^{-2} a^{-1}), mild decrease (−2,550 t km^{-2} a^{-1} ≤ CI < −1,275 t km^{-2} a^{-1}), stable (−1,275 t km^{-2} a^{-1} ≤ CI < 1,275 t km^{-2} a^{-1}), mild increase (1,275 t km^{-2} a^{-1} ≤ CI < 2,550 t km^{-2} a^{-1}), moderate increase (2,550 t km^{-2} a^{-1} ≤ CI < 3,825 t km^{-2} a^{-1}), and intensive increase (CI > 3,825 t km^{-2} a^{-1}). During 2005–2015, the most widely distributed grade was that of "stable" (with an area ratio of 82.16%), which was mainly distributed in Songpan, western Lixian, and western Wenchuan Counties. Zones with mild, moderate, and intensive decreases were discontinuously distributed in the river valleys of the Heishui and Zagunao Rivers, accounting for 4.66%, 2.23%, and

TABLE 4 Comparison of soil erosion in 2005 and 2015

Erosion intensity	2005			2015		
	Area (km^2)	Erosion rate (t km^{-2} a^{-1})	Total erosion (10^4 t)	Area (km^2)	Erosion rate (t km^{-2} a^{-1})	Total erosion (10^4 t)
Slight erosion	8,345.75	181.03	151.09	7,102.06	207.54	147.40
Mild erosion	10,595.00	1,368.64	1,450.07	11,522.75	1,362.74	1,570.25
Moderate erosion	4,582.75	3,486.59	1,597.82	5,249.88	3,471.42	1,822.45
Intensive erosion	1,064.94	5,959.08	634.60	759.31	5,777.14	438.67
Severe erosion	61.56	8,844.76	54.45	16.00	8,728.92	13.97

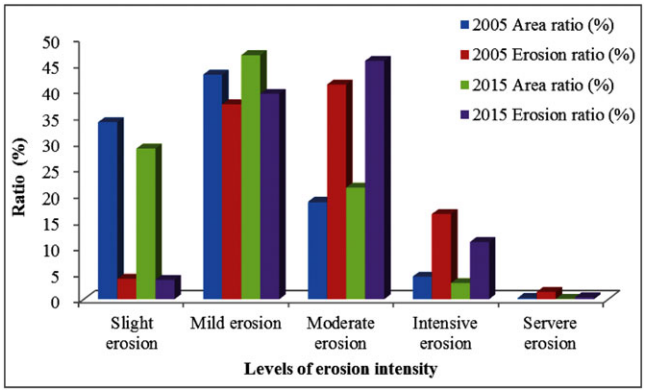

FIGURE 3 Comparisons between area ratios and erosion ratios of different erosion intensity levels [Colour figure can be viewed at wileyonlinelibrary.com]

FIGURE 5 Change trends in soil erosion intensity index for different land use types during 2005–2015 [Colour figure can be viewed at wileyonlinelibrary.com]

1.37%, respectively. In addition, zones of mild, moderate, and intensive increases were mainly concentrated in southern Maoxian and western Wenchuan Counties, where the Longmenshan Fault Zone is located.

Figure 7 shows that a significantly different change process was involved at each level of SEI. During 2005–2015, the mild erosion zone was the most stable grade with 73.50% unchanged, followed by moderate erosion (69.14% unchanged). In contrast, the severe erosion zone underwent the most dramatic change (only 16.65 unchanged) and its remaining areas changed into zones of intensive and moderate erosion. Moderate erosion was the second most stable category (69.14% unchanged), but 20.64% of this zone turned into zones of mild erosion. In total, therefore, there was a rise in the erosion intensity category of 40.56% of zones whereas 59.44% of zones remained unchanged. However, the most dramatic change occurred for the grade of severe erosion (only 16.65% unchanged), whereas the other areas changed mainly into intensive erosion zones.

4 | DISCUSSION

4.1 | Influences of land use changes on SEI

Change in land use types, as a controllable factor, has significant relationships with change of the SEI (B. Guo et al., 2012). Determining the cause of land use changes on changes in the SEI can thus provide important decision supports for use in compiling soil erosion prevention and governance strategies (Deng et al., 2008; L.

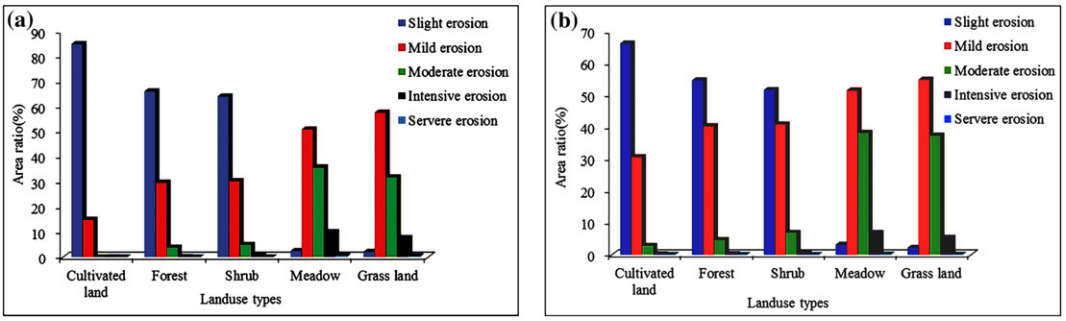

FIGURE 4 Spatial patterns of different erosion levels among land use types. (a) 2005. (b) 2015 [Colour figure can be viewed at wileyonlinelibrary.com]

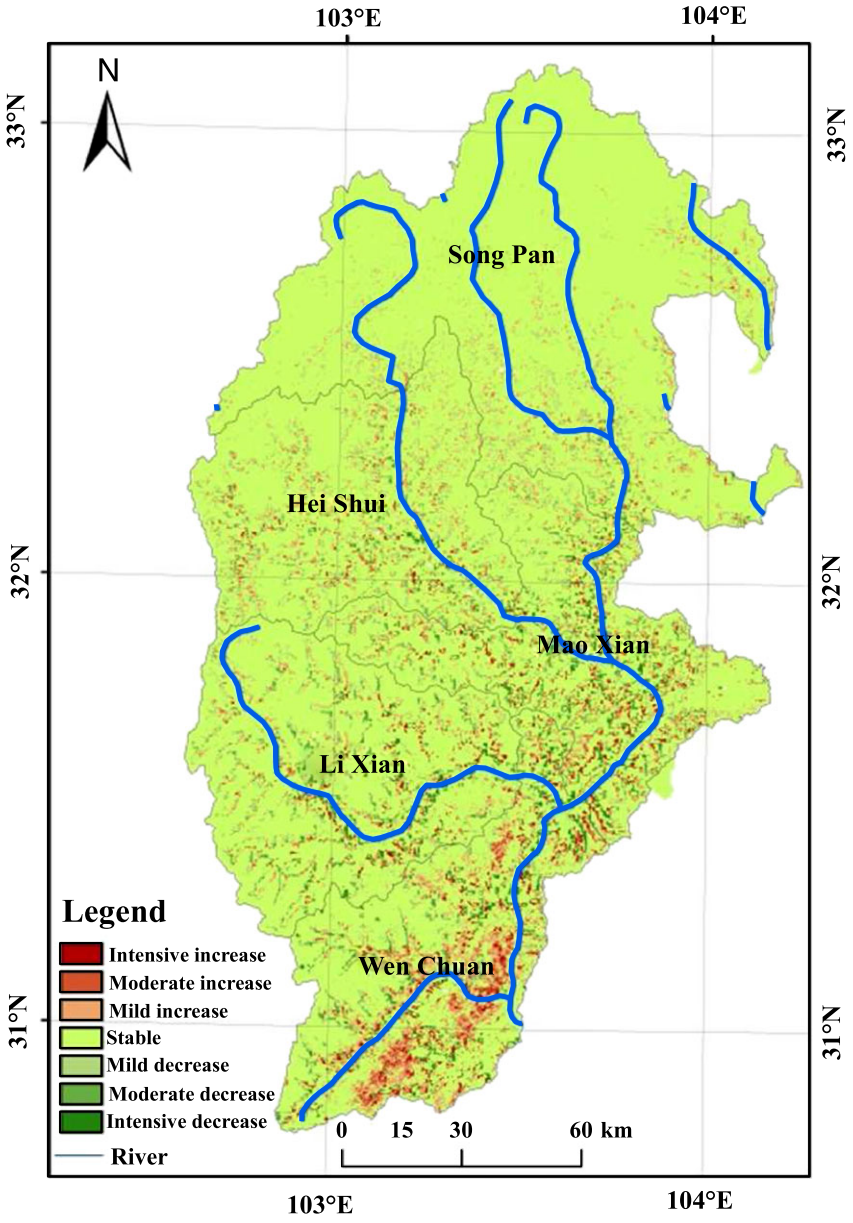

FIGURE 6 Spatial pattern of changes in soil erosion intensity during 2005–2015 [Colour figure can be viewed at wileyonlinelibrary.com]

Jiang et al., 2014). Land use changes in the upper Minjiang catchment have changed dramatically since 2000 because of the policy of returning farmland to forests and grasslands and also in relation to frequent occurrence of geological disasters (such as earthquakes, landslides, and debris flows; A. N. Li et al., 2006; L. F. Xu et al., 2013).

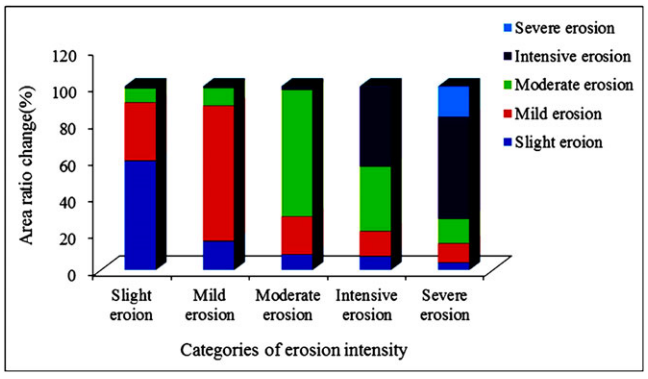

FIGURE 7 Change matrix for areas of different soil erosion grades in the upper Minjiang catchment during 2005–2015 [Colour figure can be viewed at wileyonlinelibrary.com]

To further clarify the impacts of different land use changes on soil erosion, we divide changes in land use into two categories: (a) cultivated land turned into forest and grassland and (b) forest and grassland turned into bare land, cultivated land, and sparse grassland (Figure 8). In 2005, the erosion intensity of cultivated land was 1,210.29 t km^{-2} a^{-1} with an erosion amount of 36.38 × 10^4 t, whereas forest and grassland returned from cultivated had an erosion modulus of 437.8 t km^{-2} a^{-1} with an erosion amount of 13.16 × 10^4 t. In detail, the zones of mild, moderate, and intensive erosion were widely distributed in regions dominated by cultivated land in 2005. However, by 2015, the largest erosion level was that of "slight erosion," accounting for 86.93% of the region that had been changed from cultivated land (Figure 8). Therefore, returning cultivated land to forest and grassland greatly reduced the erosion intensity and erosion amount by 772.49 t km^{-2} a^{-1} and 23.22 × 10^4 t, which thus significantly improved soil function and water conversation.

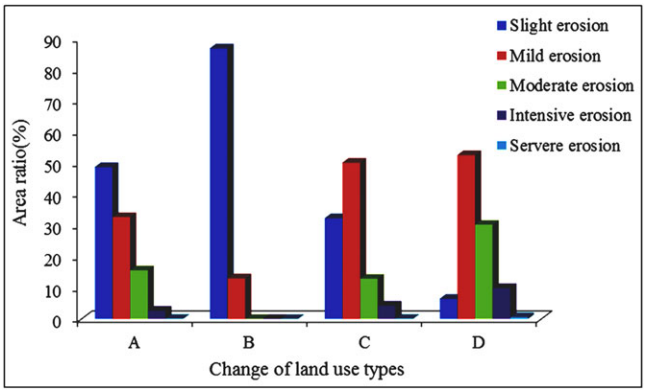

FIGURE 8 Comparison of soil erosion intensity in changed land use during 2005–2015. Column A refers to cultivated land for 2005; B refers to forest and grassland returned from cultivated land by 2015; C refers to forest and grassland in 2005; and D refers to bare land and sparse grassland changes from forest and grassland for 2015 [Colour figure can be viewed at wileyonlinelibrary.com]

For forest and grassland areas turned into bare land, cultivated land, and sparse grassland, the erosion intensity for grassland and forest was 1,435.05 t km^{-2} a^{-1} in 2005, with an erosion amount of 33.75 × 10^4 t. However, bare land, cultivated land, and sparse grassland that had been changed from forest and grassland had an erosion modulus of 2,496.03 t km^{-2} a^{-1} with an erosion amount of 58.70 × 10^4 t. Moreover, during 2005–2015, there was an increased trend in mild, moderate, and intensive erosion but a large reduction in areas of slight erosion. Forest and grasslands are mostly distributed in alpine gorges with steep slopes and within geological fracture zones, and thus the surface cover suffers serious damage from geologic hazards, such as earthquakes, landslides, and debris flow; this occurred particularly during the Wenchuan earthquake (M_s 8.0) and the Lushan earthquake (M_s 7.0; L. Q. Chen, Wu, Yang, & Zhang, 2012; B. T. Liu et al., 2016). During 2005–2015, these geologic hazards aggravated the condition of soil erosion and enlarged the erosion intensity and amount by 1,060.98 t km^{-2} a^{-1} and 24.95 × 10^4 t. Therefore, strengthening the ability to prevent geologic hazards and reconstruct areas post-disaster is of great importance when improving the condition of soil and conserving water.

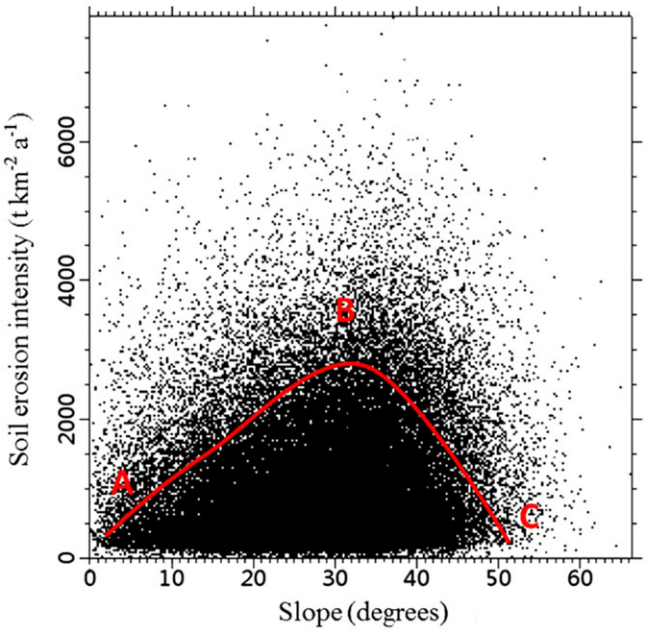

FIGURE 9 Relationship between soil erosion intensity and slope [Colour figure can be viewed at wileyonlinelibrary.com]

4.2 | Relationship between slope and SEI

Slope plays an important role in influencing the spatial patterns of SEI (B. Guo et al., 2012). Middle and high steep cliffs are widely distributed in the upper Minjiang catchment, and it is important to quantitatively evaluate the relationship between slope and the SEI to prevent soil erosion in study area (Fang et al., 2014; A. N. Li et al., 2006). As shown in Figure 9, the SEI–slope curve shows a single peak. In Section AB of the curve (slope < 35°), the SEI increases with an increase in slope gradient; this is because the slope has a significantly positive effect on the process of soil loss through erosion (B. T. Liu et al., 2016). The greater the gradient and length of a slope, the larger the runoff energy and the greater the soil loss (L. Jiang et al., 2014; Khaleghpanah et al., 2016). However, in Section BC of the curve, there is a negative relationship between the erosion intensity and slope; this is because the process of soil formation is slow in steep slope zones and the soil layer is shallow (L. Q. Chen et al., 2012; Y. Q. Xu et al., 2008). Thus, zones with slopes of >35° in the upper Minjiang catchment are not suitable for vegetation growth, and regions with slope of <35° are areas that require crucial soil loss control.

4.3 | Relationship between plant types, VC, and SEI

The below-ground parts of vegetation can not only enhance the stability of soil mass but also reduce the scouring influences of runoff. Meanwhile, the above-ground parts of the plant can decrease the erosive force of precipitation (Cai, Ding, Shi, Huang, & Zhang, 2000; Shi et al., 2002). However, the relationship between VC and erosion intensity among different plant types differs significantly (Figure 10). Forest and grassland are widely distributed in the upper Minjiang catchment, accounting for 51% of the entire study region (A. N. Li et al., 2006; L. F. Xu et al., 2013). Therefore, the influences of VC on the soil erosion in forest and grassland are analyzed, respectively.

As shown in Figure 11a, for grassland, (a) vegetation has a negative relation with soil erosion in Section AB of the curve (VC < 0.35) because of the protective function of vegetation on ground soil. (b) However, in Section BC of the curve (0.35 ≤ VC < 0.75), the SEI increases with an expansion of VC, which is inconsistent with the inhibitive influences of vegetation on soil loss. The slope is then extracted to analyze its effect on the SEI in zone (0.35 ≤ VC < 0.75) for grassland. Figure 11b shows that the slope in zone (0.35 ≤ VC < 0.75) ranges from 10° to 40° and that the SEI increases with an enlargement of the slope. Therefore, for grassland with 0.35 ≤ VC < 0.75, slope plays a dominant role in effecting the SEI. (c) In Section CD of the curve (VC ≥ 0.75), there is a positive relationship between the SEI and VC, which indicates that the VC of grassland plays a leading role in the processes involved in soil and water loss.

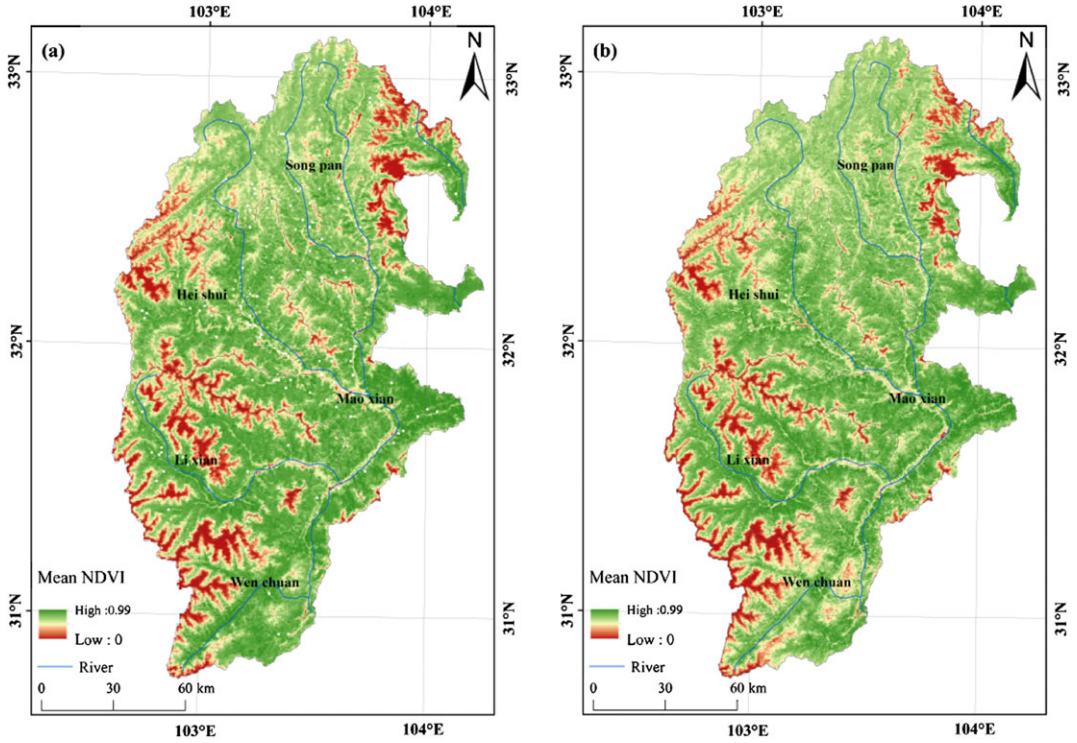

FIGURE 10 Annually mean NDVI of the upper Minjiang catchment. (a) Annually mean NDVI in 2005. (b) Annually mean NDVI in 2015 [Colour figure can be viewed at wileyonlinelibrary.com]

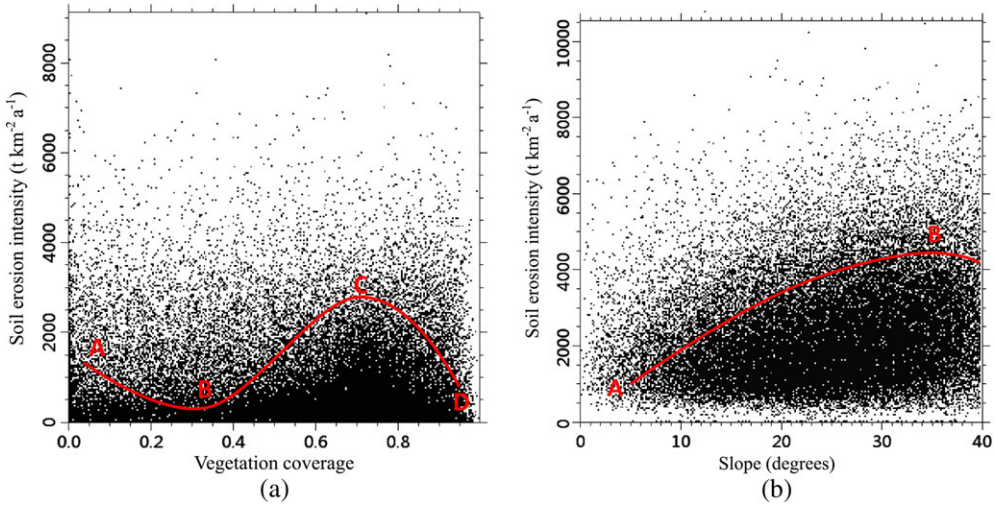

FIGURE 11 Relationships between soil erosion intensity and vegetation coverage for grassland. (a) Relationships between soil erosion intensity and vegetation coverage for grassland. (b) Effects of slope on soil erosion intensity for 0.35 ≤ VC < 0.75 [Colour figure can be viewed at wileyonlinelibrary.com]

As shown in Figure 12a, for forestland, (a) in section AB of the curve (VC < 0.8), the SEI increases with VC. In consideration of the inconsistency between the change trend and soil conversation in forests, slope zones with VC < 0.8 are extracted to explore this problem. Figure 12b shows that the slope of the zone (VC < 0.8) has a positive relation with the SEI. Therefore, for forestland with VC < 0.8, the slope plays a dominant role in effecting the SEI. (b) In Section BC of the curve (VC > 0.8), the SEI decreases with expansion of the VC, which indicates that forestland with VC > 0.8 plays a more important role in the process of soil erosion than slope.

Based on the above analysis of the relationships between plant type, VC, and SEI, grassland is thus considered to be more effective in conserving soil and water than forestland in the upper Minjiang catchment where there is steep terrain. Therefore, grassland should be the focus of plans when implementing policies for returning farmland to forests and grassland.

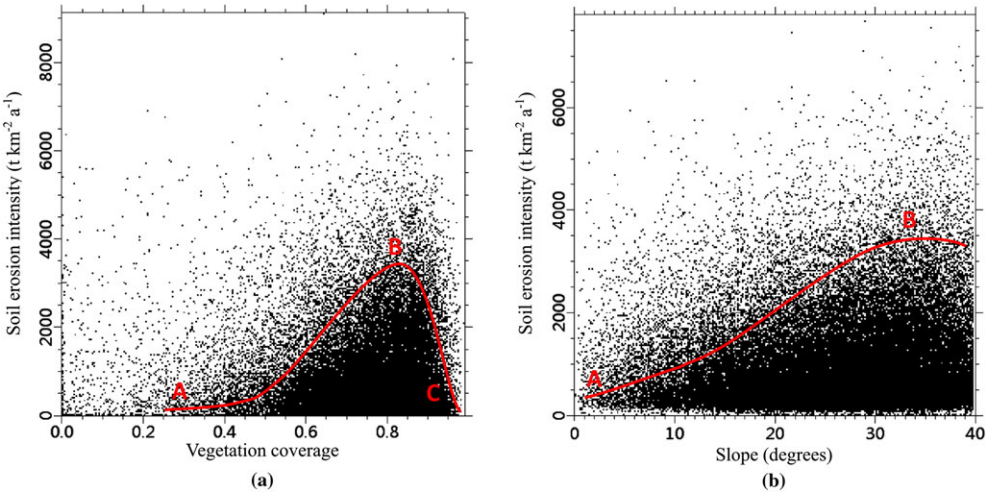

FIGURE 12 Relationships between soil erosion intensity and vegetation coverage for forestland. (a) Relationships between soil erosion intensity and vegetation coverage for forest. (b) Effects of slope on soil erosion intensity for VC < 0.8 [Colour figure can be viewed at wileyonlinelibrary.com]

5 | CONCLUSION

The unique geographical conditions, steep terrain, and widely distributed forests and grassland are considered in the upper Minjiang catchment, and improved methods for *K*, *LS*, and *C* are introduced to establish the soil loss equation for this area, based on RS and GIS. Spatial–temporal change patterns in the SEI and its driving mechanisms are then analyzed and discussed. The main results are as follows:

1. The soil erosion moduli for the upper Minjiang catchment in 2005 and 2015 are 1,577.29 and 1,619.77 t km^{-2} a^{-1}, both of which belong to the level of "mild erosion." In addition, the total amounts of soil eroded in 2005 and 2015 were 3,888 × 10^4 t and 3,992 × 10^4 t, respectively.
2. Zones of slight and mild erosion were widely distributed in the northern part of the study region, whereas the intensive and severe erosion zones were mostly concentrated in Wenchuan County and the lower reaches of the Heishui and Zagunao Rivers.
3. During 2005–2015, the change in SEI showed a trend of "overall stability, local deterioration," whereas zones of mild, moderate, and intensive increase were mainly concentrated in southern Maoxian and western Wenchuan Counties.
4. Returning cultivated land to forest and grassland has greatly reduced the amount and intensity of erosion, although geologic hazards have aggravated the soil erosion condition. Zones with slopes of <35° have a positive relationship with SEI and are thus crucial control areas for soil preservation and restricting loss. In addition, grasslands are more effective in conserving soil and water than forestland in the upper Minjiang catchment in areas of steep terrain.

ACKNOWLEDGMENTS

This work was supported by the Open Fund of Key Laboratory of Geographic Information Science (Ministry of Education), East China Normal University (Grant KLGIS2017A02), the Open Fund of Key Laboratory for Digital Land and Resources of Jiangxi Province, East China University of Technology (Grant DLLJ201709), the Open Fund of Key Laboratory for National Geographic Census and Monitoring, National Administration of Surveying, Mapping and Geoinformation (Grant 2016NGCM02), and the Project of Hubei Key Laboratory of Regional Development and Environmental Response (Hubei University) (Grant 2017(B)003).

ORCID

Bing Guo http://orcid.org/0000-0003-0042-9643

REFERENCES

Al-Hamdan, M. Z., Oduor, P., Flores, A. I., Kotikot, S. M., Mugo, R., Ababu, J., & Farah, H. (2017). Evaluating land cover changes in Eastern and Southern Africa from 2000 to 2010 using validated Landsat and MODIS data. *International Journal of Applied Earth Observation and Geoinformation*, *62*, 8–26. https://doi.org/10.1016/j.jag.2017.04.007

Baigorria, G. A., & Romero, C. C. (2007). Assessment of erosion hotspots in a watershed: Integrating the WEPP model and GIS in a case study in the Peruvian Andes. *Environmental Modelling & Software*, *22*, 1175–1183. https://doi.org/10.1016/j.envsoft.2006.06.012

Brooks, E. S., Dobre, M., Elliot, W. J., Wu, J. Q., & Boll, J. (2016). Watershed-scale evaluation of the Water Erosion Prediction Project (WEPP) model in the Lake Tahoe basin. *Journal of Hydrology*, *533*, 389–402. https://doi.org/10.1016/j.jhydrol.2015.12.004

Cai, C. F., Ding, S. W., Shi, Z. H., Huang, L., & Zhang, G. Y. (2000). Study of applying USLE and geographical information system IDRISI to predict soil erosion in small watershed. *Journal of Soil and Water Conservation*, *14*, 19–24. https://doi.org/10.3321/j.issn:1009-2242.2000.02.005

Chen, H., Oguchi, T., & Wu, P. (2017). Assessment for soil loss by using a scheme of alterative sub-models based on the RUSLE in a Karst Basin of Southwest China. *Journal of Integrative Agriculture*, *16*, 377–388. https://doi.org/10.1016/S2095-3119(16)61507-1

Chen, L. Q., Wu, F. Z., Yang, W. Q., & Zhang, J. (2012). A comparison on ecosystem services before/after "5.12" Wenchuan earthquake. *Acta Ecologica Sinica*, *32*, 271–273. https://doi.org/10.1016/j.chnaes.2012.07.002

Cheng, L., Yang, Q. K., Xie, H. X., Wang, C. M., & Guo, W. L. (2009). GIS and CSLE based quantitative assessment of soil erosion in Shaanxi, China.

Journal of Soil and Water Conservation, *23*, 62–66. https://doi.org/10.3321/j.issn:1009-2242.2009.05.013

Dabral, P. P., Baithuri, N., & Pandey, A. (2008). Soil erosion assessment in a hilly catchment of North Eastern India using USLE, GIS and remote sensing. *Water Resources Management*, *22*, 1783–1798. https://doi.org/10.1007/s11269-008-9253-9

Deng, Y. L., Meng, Z. X., Wang, Y. K., & Liu, W. L. (2008). Study on soil erosion changes and controlling strategy in the Minjiang River Valley. *Journal of Soil and Water Conservation*, *22*, 56–60 https://doi.org/10.3321/j.issn:1009-2242. 2008.05.013

Fang, Y. P., Fan, J., Shen, M. Y., & Song, M. Q. (2014). Sensitivity of livelihood strategy to livelihood capital in mountain areas: Empirical analysis based on different settlements in the upper Mianjiang catchment, China. *Ecological Indicators*, *38*, 225–235. https://doi.org/10.1016/j.ecolind.2013.11.007

Fu, B. J., Zhao, W. W., Chen, L. D., Zhang, Q. J., Lü, Y. H., Gulinck, H., & Poesen, J. (2005). Assessment of soil erosion at large watershed scale using RUSLE and GIS: A case study in the Loess Plateau of China. *Land Degradation & Development*, *16*, 73–85. https://doi.org/10.1002/ldr.646

Ganasri, B. P., & Ramesh, H. (2016). Assessment of soil erosion by RUSLE model using remote sensing and GIS—A case study of Nethravathi Basin. *Geoscience Frontiers*, *7*, 953–961. https://doi.org/10.1016/j.gsf.2015.10.007

Ge, Y. G., Cui, P., Lin, Y. M., Zhuang, J. Q., & Jia, S. W. (2014). Soil erosion evaluation and prediction approach using ^{137}Cs, RS, and GIS in Xiaojiang River basin of China. *Journal of Remote Sensing*, *18*, 887–901. https://doi.org/10.11834/jrs.20143128.

Guo, B., Tao, H. P., Liu, B. T., & Jiang, L. (2012). Characteristics and analysis of soil erosion in Li country after Wenchuan earthquake based on GIS and USLE. *Transactions of the Chinese Society of Agricultural Engineering (Transactions of the CSAE)*, *28*, 118–126. https://doi.org/10.3969/j.issn.1002-6819.2012.14.019

Guo, Q. K., Liu, B. Y., Xie, Y., Liu, Y. N., & Yin, S. Q. (2015). Estimation of USLE crop and management factor values for crop rotation systems in China. *Journal of Integrative Agriculture*, *14*, 1877–1888. https://doi.org/10.1016/S2095-3119(15)61097-8

Hong, C., Yanqiong, L., Shaowei, Z., Ling, W., Fei, H., Jun, L., & Changlong, M. (2007). Determination of species-area relationships and minimum sampling area for the shrub communities in the arid valley in the upper reach of the Minjiang River, China. *Acta Ecologica Sinica*, *27*, 1818–1825. https://doi.org/10.1016/S1872-2032(07)60044-4

Jiang, L., Bian, J. H., Li, A. N., Lei, G. B., Nan, X., Feng, W. L., & Li, G. (2014). Spatial-temporal changes of soil erosion in the upper reaches of Minjiang River from 2000 to 2010. *Journal of Soil and Water Conservation*, *28*, 19–25. https://doi.org/10.3969/j.issn.1009-2242.2014.01.004

Jiang, Z. S., & Zheng, F. L. (2004). Water erosion prediction model at hillslope scale. *Journal of Soil and Water Conservation*, *18*, 66–69. https://doi.org/10.3321/j.issn:1009-2242.2004.01.017

Khaleghpanah, N., Shorafa, M., Asadi, H., Gorji, M., & Davari, M. (2016). Modeling soil loss at plot scale with EUROSEM and RUSLE2 at stony soils of Khamesan watershed, Iran. *Catena*, *147*, 773–788. https://doi.org/10.1016/j.catena.2016.08.039

Kinnell, P. I. A. (2017). A comparison of the abilities of the USLE-M, RUSLE2 and WEPP to model event erosion from bare fallow areas. *Science of the Total Environment*, *596–597*, 32–42. https://doi.org/10.1016/j.scitotenv.2017.04.046

Koiter, A. J., Owens, P. N., Petticrew, E. L., & Lobb, D. A. (2017). The role of soil surface properties on the particle size and carbon selectivity of interrill erosion in agricultural landscapes. *Catena*, *153*, 194–206. https://doi.org/10.1016/j.catena.2017.01.024

Lee, G. S., & Lee, K. H. (2006). Scaling effect for estimating soil loss in the RUSLE model using remotely sensed geospatial data in Korea. *Journal of Hydrology and Earth System Sciences*, *3*, 135–157 https://doi.org/10.5194/hessd-3-135-2006 · Source: OAI

Li, A. N., Wang, A. S., Liang, S. L., & Zhou, W. C. (2006). Eco-environmental vulnerability evaluation in mountainous region using remote sensing and GIS—A case study in the upper reaches of Minjiang River, China. *Ecological Modelling*, *192*, 175–187. https://doi.org/10.1016/j.ecolmodel.2005.07.005

Li, Z. W., Liu, C., Dong, Y. T., Chang, X. F., Nie, X. D., Liu, L., … Zeng, G. M. (2017). Response of soil organic carbon and nitrogen stocks to soil erosion and land use types in the Loess hilly–gully region of China. *Soil and Tillage Research*, *166*, 1–9. https://doi.org/10.1016/j.still.2016.10.004

Liu, B. T., Song, C. F., Shi, Z., & Tao, H. P. (2016). Soil loss equation of Lushan earthquake area. *Journal of Yangtze River Scientific Research Institute*, *33*, 15–19. https://doi.org/10.11988/ckyyb.20140674

Liu, B. Y., Bi, X. G., & Fu, S. H. (2010). *Soil loss equation of Beijing*. Beijing: Science Press.

Liu, K., Tang, G. A., Zhu, A. X., Yang, J. Y., & Song, X. D. (2015). Regional-scale calculation of the LS factor using parallel processing. *Computers & Geosciences*, *78*, 110–122. https://doi.org/10.1016/j.cageo.2015.02.001

Liu, Y., Li, C. Y., & Long, Y. (2009). Relationship between agroforest landscape and soil erosion intensity in Minjiang headwater region. *Transaction of the Chinese Society of Agricultural Engineering (Transactions of the CSAE)*, *25*, 232–236. https://doi.org/10.3969/j.issn.1002-6819.2009.07.042

Mattheus, C. R., & Norton, M. S. (2015). Comparison of pond-sedimentation data with a GIS-based USLE model of sediment yield for a small forested urban watershed. *Anthropocene*, *2*, 89–101. https://doi.org/10.1016/j.ancene.2013.10.003

Prasannakumar, V., Vijith, H., Abinod, S., & Geetha, N. (2012). Estimation of soil erosion risk within a small mountainous sub-watershed in Kerala, India, using Revised Universal Soil Loss Equation (RUSLE) and geo-information technology. *Geoscience Frontiers*, *3*, 209–215. https://doi.org/10.1016/j.gsf.2011.11.003

Shi, Z. H., Cai, C. F., Ding, S. W., Li, C. Y., & Wang, T. W. (2002). Soil conservation planning at small watershed level using GIS-based Revised Universal Soil Loss Equation (RUSLE). *Transactions of the Chinese Society of Agricultural Engineering (Transactions of the CSAE)*, *18*, 172–175. https://doi.org/10.3321/j.issn:1002-6819.2002.04.042

Tamene, L., Park, S. J., Dikau, R., & Vlek, P. L. G. (2006). Analysis of factors determining sediment yield variability in the highlands of Northern Ethiopia. *Geomorphology*, *76*, 76–91. https://doi.org/10.1016/j.geomorph.2005.10.007

Vanwalleghem, T., Gómez, J. A., Infante, J. A., de Molina, M. G., Vanderlinden, K., Guzmán, G., … Giráldez, J. V. (2017). Impact of historical land use and soil management change on soil erosion and agricultural sustainability during the Anthropocene. *Anthropocene*, *17*, 13–29. https://doi.org/10.1016/j.ancene.2017.01.002

Wei, S. C., Zhang, X. P., McLaughlin, N. B., Chen, X. W., Jia, X. X., & Liang, A. Z. (2017). Impact of soil water erosion processes on catchment export of soil aggregates and associated SOC. *Geoderma*, *294*, 63–69. https://doi.org/10.1016/j.geoderma.2017.01.021

Xiao, H., Liu, G., Liu, P. L., Zheng, F. L., Zhang, J. Q., & Hu, F. N. (2017). Developing equations to explore relationships between aggregate stability and erodibility in Ultisols of subtropical China. *Catena*, *157*, 279–285. https://doi.org/10.1016/j.catena.2017.05.032

Xie, Y., Yin, S. Q., Liu, B. Y., Nearing, M. A., & Zhao, Y. (2016). Models for estimating daily rainfall erosivity in China. *Journal of Hydrology*, *535*, 547–558. https://doi.org/10.1016/j.jhydrol.2016.02.020

Xu, L. F., Xu, Y. G., & Meng, X. W. (2013). Risk assessment of soil erosion in different rainfall scenarios by RUSLE model coupled with information diffusion model: A case study of Bohai Rim, China. *Catena*, *100*, 74–82. https://doi.org/10.1016/j.catena.2012.08.012

Xu, Y. Q., Shao, X. M., Kong, X. B., Peng, J., & Cai, Y. L. (2008). Adapting the RUSLE and GIS to model soil erosion risk in a mountains karst watershed, Guizhou Province, China. *Environmental Monitoring and*

Assessment, *141*, 275–286. https://doi.org/10.1007/s10661-007-9894-9

Xu, Y. Q., Shao, X. M., & Peng, J. (2009). Assessment of soil erosion using RUSLE and GIS: A case study of the Maotiao River watershed, Guizhou Province, China. *Environmental Geology*, *56*, 1643–1652. https://doi.org/10.1007/s00254-008-1261-9

Zhang, K. L., Shu, A. P., Xu, X. L., Yang, Q. K., & Yu, B. (2008). Soil erodibility and its estimation for agricultural soils in China. *Journal of Arid Environments*, *72*, 1002–1011 https://doi.org/10.1016/j.jaridenv.2007.11.018 · source: OAI

Zhang, W. B., & Liu, B. Y. (2003). Development of Chinese soil loss equation information system based on GIS. *Journal of Soil and Water Conservation*, *17*, 89–92. https://doi.org/10.3321/j.issn:1009-2242.2003.02.025

Zhang, W. G., Hu, Y. M., Hu, J. C., Chang, Y., Zhang, J., & Liu, M. (2008). Impacts of land-use change on mammal diversity in the upper reaches of Minjiang River, China: Implications for biodiversity conservation planning. *Landscape and Urban Planning*, *85*, 195–204. https://doi.org/10.1016/j.landurbplan.2007.11.006

How to cite this article: Guo B, Yang G, Zhang F, Han F, Liu C. Dynamic monitoring of soil erosion in the upper Minjiang catchment using an improved soil loss equation based on remote sensing and geographic information system. *Land Degrad Dev*. 2018;29:521–533. https://doi.org/10.1002/ldr.2882